Moisture supply to the Atacama Desert by Atmospheric Rivers

Böhm[1], C., M. Reyers[1], and S. Crewell[1]
[1] *Institute of Geophysics and Meteorology, University of Cologne*

Earth – Evolution at the dry limit

1. Introduction

In hyperarid regions, such as the Atacama desert in northern Chile, the very rarely occurring precipitation events can leave long lasting traces in the landscape.

- The goal of the Collaborative Research Center "Earth – Evolution at the dry limit" funded by German Science Foundation is to understand the sources, pathways and variability of moisture supplied to the Atacama desert.

- We investigate the situations when atmospheric rivers (AR) occur in that region and their contribution to the overall precipitation.

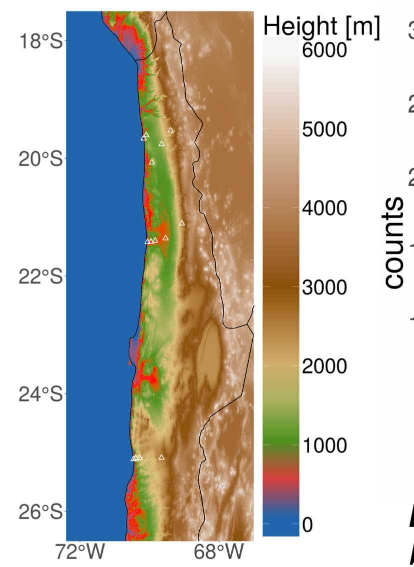

***Fig. 1**: Topography of northern Chile derived from the Shuttle Radar Topographic mission (SRTM) data set.*

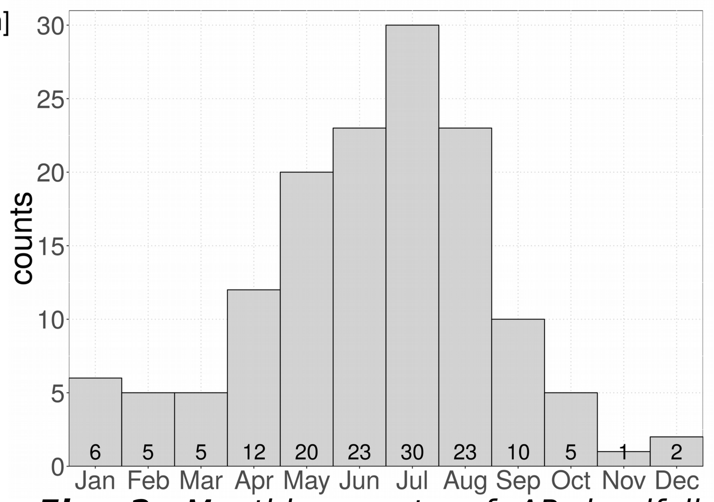

***Fig. 2**: Monthly counts of AR landfalls between 16.5°S and 31.5°S. AR shapes and landfall locations are according to Guan and Waliser (2015). In the considered period of 38 years (1978-2015) a total of 142 AR landfalls are found. Most (76 or 54%) occur during winter (JJA).*

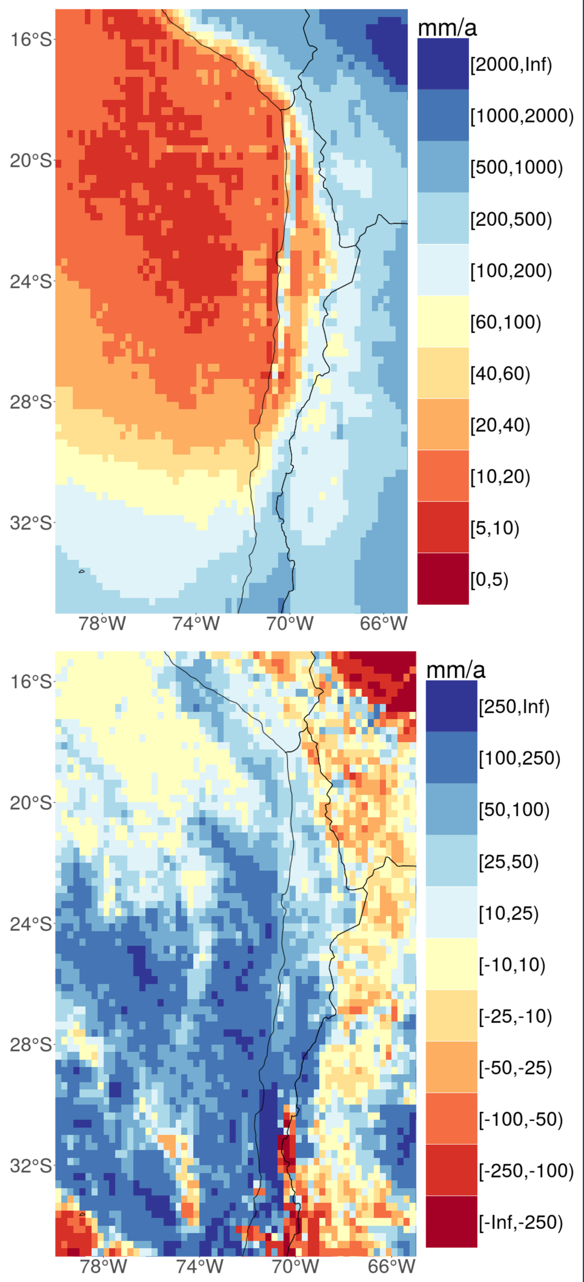

***Fig. 3**: Precipitation rate (1998-2015) derived from TRMM. Top: climatology. Bottom: Deviation from the climatology for days when AR made landfall between 16.5°S and 31.5°S. For the anomaly only the winter season (JJA) is considered which is the season with highest AR landfall frequency (see Fig. 2).*

2. Data

***Tab. 1**: Description of the data sets which are applied in this study.*

Acronym	Data	Period	Description
AR	Atmospheric Rivers	1978-2015	Shape and landfall locations; resolution: 0.75° Source: Guan and Waliser (2015)
ERA-Int	ECMWF Reanalysis ERA-Int	1978-2015	500hPa/700hPa geopotential, 500hPa specific humidity, sea level pressure; resolution: 0.75°
TRMM	Tropical Rainfall Measuring Mission	1998-2015	Product: 3B42; Daily accumulated precipitation; resolution: 0.25°
MODIS	Moder Imaging Spectroradiometer	2003-2017	MOD35_L2/MYD35_L2 (Terra/Aqua), cloud mask, resolution: 1km
WRF	Weather Research and Forecasting Model	20-26 May 2015	Relative humidity, precipitation, integrated water vapor (IWV) and transport (IVT), 3D wind; resolution: 10km, 44 vert. levels, hourly

3. AR induced atmospheric anomalies

Out of 185 AR landfalls detected in the Atacama 142 different days are identified and corresponding AR composites are studied in this section.

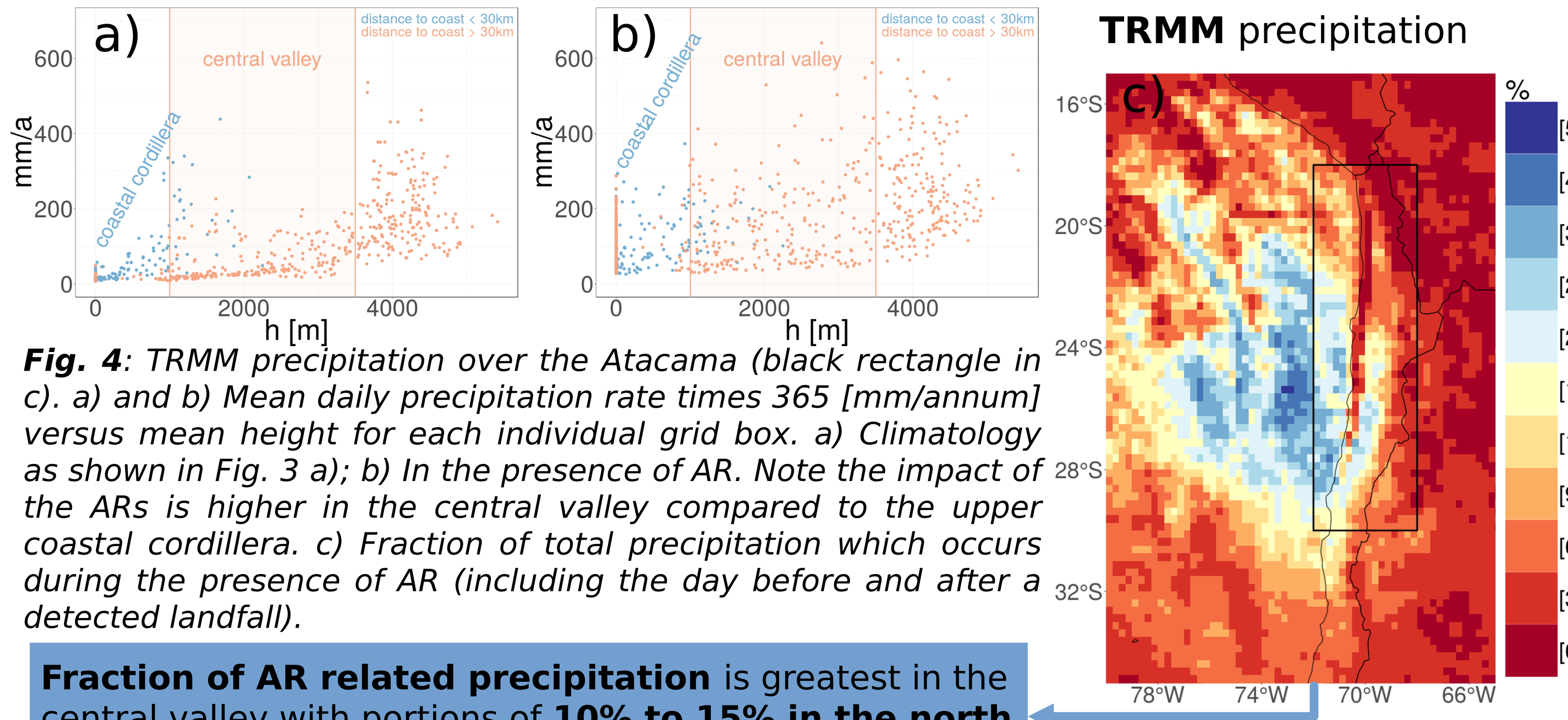

***Fig. 4**: TRMM precipitation over the Atacama (black rectangle in c). a) and b) Mean daily precipitation rate times 365 [mm/annum] versus mean height for each individual grid box. a) Climatology as shown in Fig. 3 a); b) In the presence of AR. Note the impact of the ARs is higher in the central valley compared to the upper coastal cordillera. c) Fraction of total precipitation which occurs during the presence of AR (including the day before and after a detected landfall).*

Fraction of AR related precipitation is greatest in the central valley with portions of **10% to 15% in the north** (20°S-24°S) and **20% to 30% in the south** (24°S-30°S).

ERA-Int surface pressure, geopotential, specific humidity

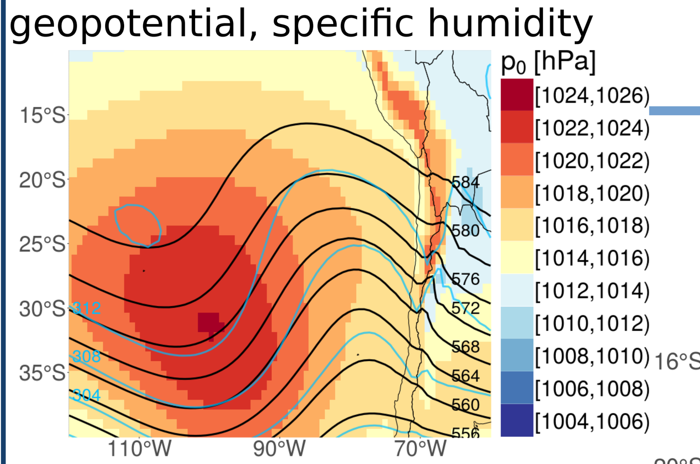

***Fig. 5**: ERA-Int AR composite of sea level pressure (color), and geopotential in 700 hPa (blue contour lines) and in 500 hPa (black contour lines). Values given in gpdam.*

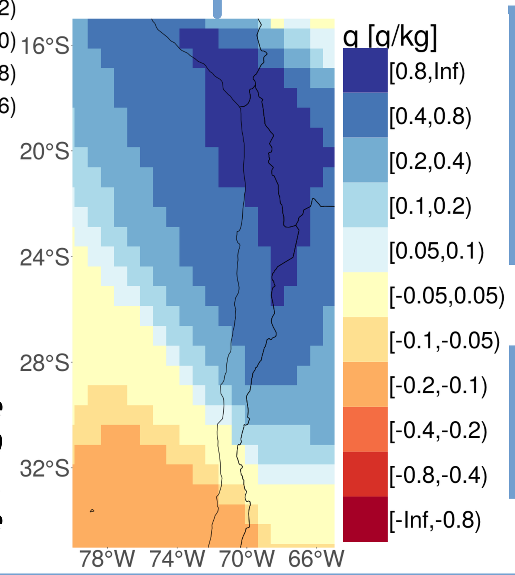

***Fig. 6**: ERA-Int AR composite anomaly of specific humidity in 500 hPa. For each day with an AR landfall, all four daily time steps are considered.*

Trough is only apparent above 850hPa, so that no surface front appears. Hence, the moisture band of the AR is well above and independent of the maritime boundary layer.

→ **moisture** can be **transported** across the coastal cordillera **into the dry core of the Atacama**

→ cloud layer and maritime boundary layer decouple

→ indicates **weaker stability during AR condition** (T inversion)

Cloud cover increases over land and decreases over ocean during presence of AR.

MODIS cloud cover

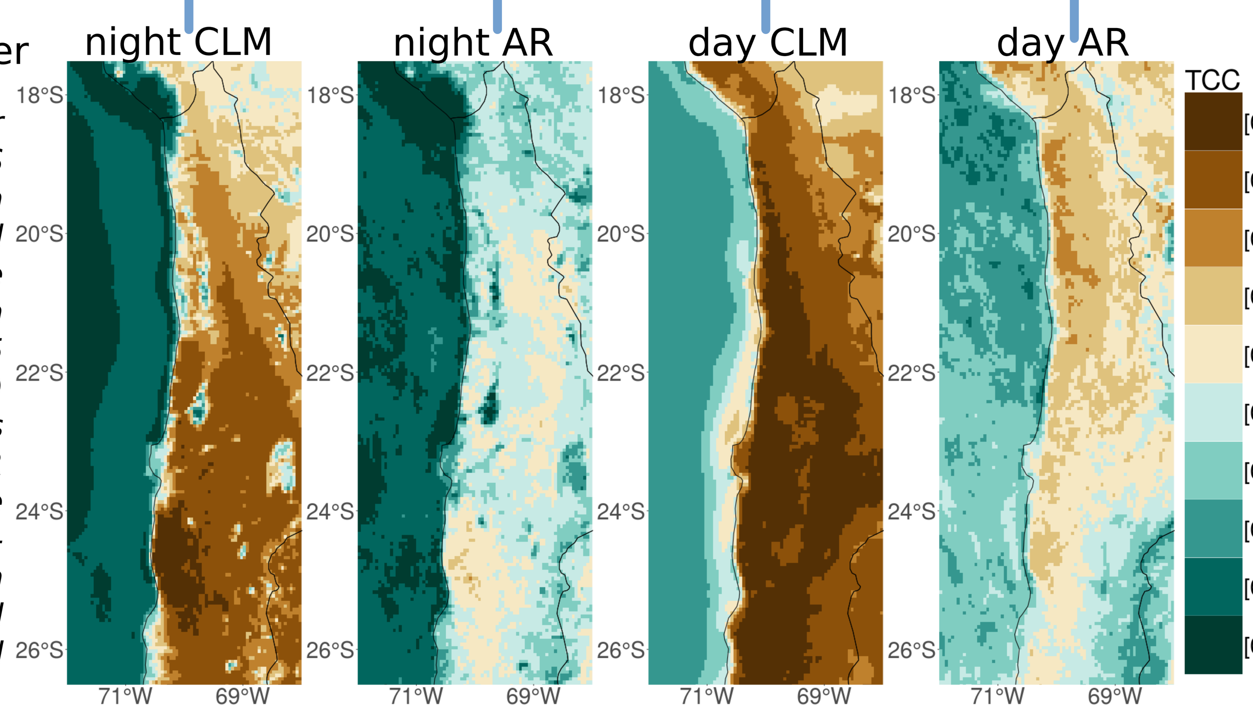

***Fig. 7**: Cloud cover derived from MODIS cloud mask. Data from individual overpasses are spatially averaged on a 0.05° grid. The 15 year (2003-2017) climatology (CLM) is compared to the AR composite. Shown are results from the Aqua-MODIS with overpasses around 1:30p.m. (day) and 1:30a.m. (night).*

4. Atmospheric River landfall on 25 May 2015

For this particular AR landfall we utilize a WRF simulation (see Tab. 1) to investigate the spatial and temporal development of the moisture ahead of the Atacama coast.

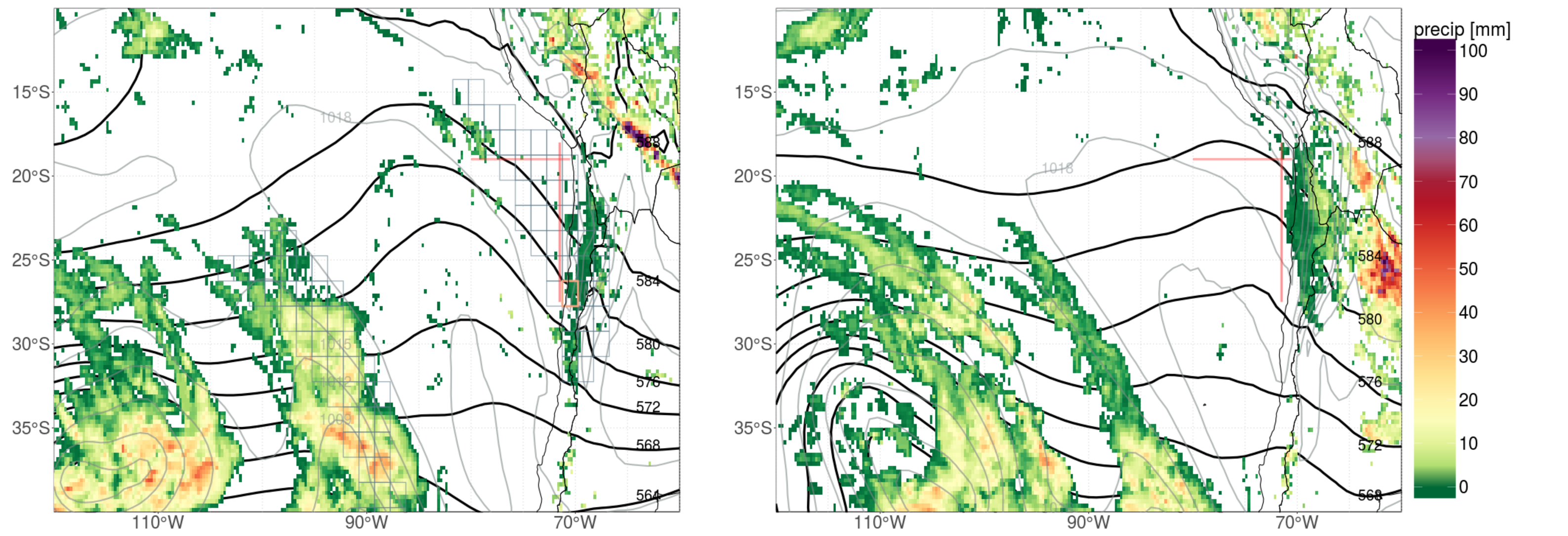

***Fig. 8**: Conditions on 25 May, 18 UTC (left) and 26 May, 12 UTC (right). Color: daily precipitation [mm] (TRMM), black lines: isohypses in 500hPa [gpdam] (ERA-Int), gray lines: isobars of mean sea level pressure [hPa] (ERA-Int), gray raster and orange rectangle: AR shape and landfall location, respectively, according to Guan and Waliser (2015), orange lines: locations of cross section for Fig. 10.*

Between 1km and 2km (~850hPa) the wind direction reverses, with southeast wind below and northwest wind above.

(Almost) saturated moisture layers above 3km to 4km.

At the beginning of the AR arrival convective boundary layer clouds only form further west. As the AR approaches the coast convective cells are also apparent further east.

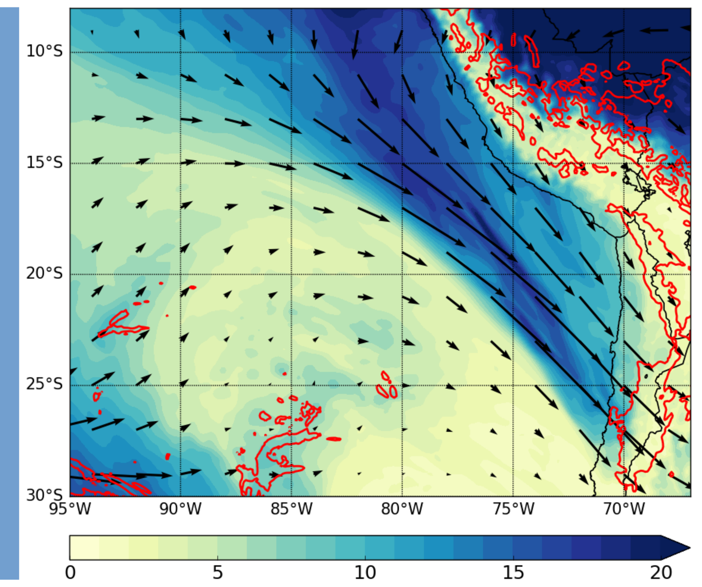

***Fig. 9**: WRF model output: IWV [kg/m²] (color) and IVT (arrows) at the time of an AR landfall in the Atacama (25 May, 18 UTC). Integration excludes lowest 10 model levels (up to 850 hPa). Red lines represent 2mm isohyet accumulated over 25-26 May.*

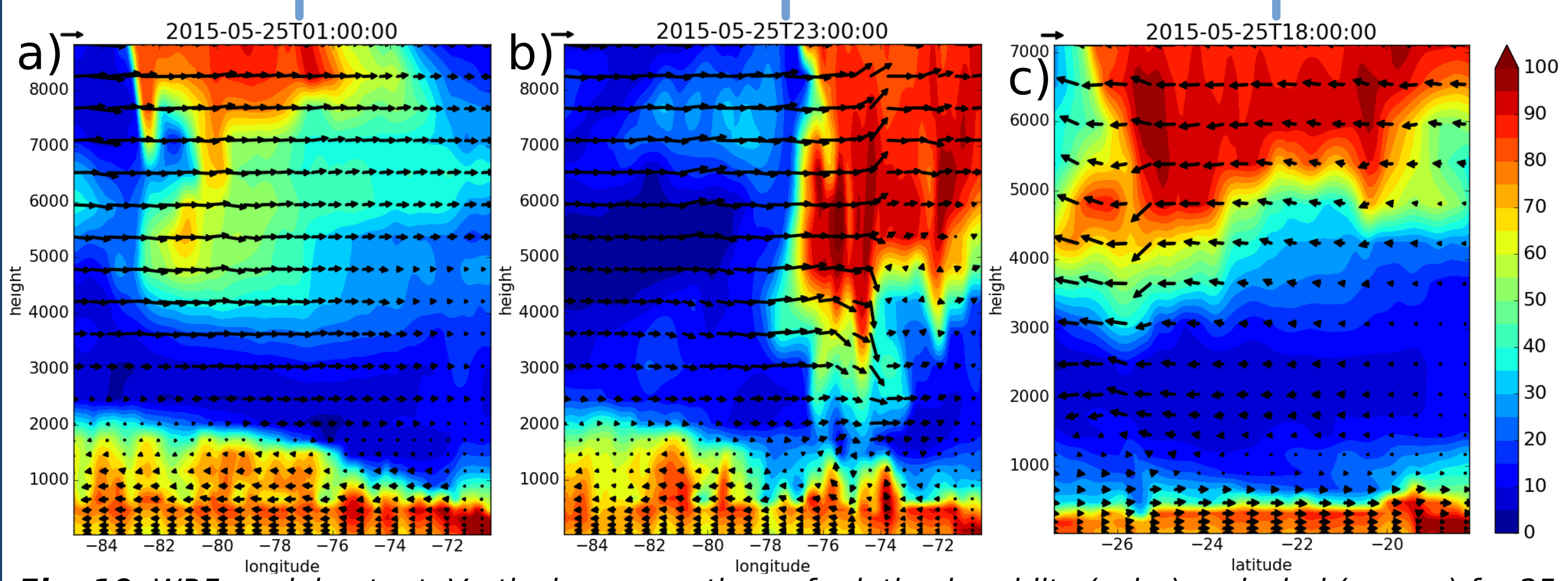

***Fig. 10**: WRF model output: Vertical cross sections of relative humidity (color) and wind (arrows) for 25 May. Zonal cross section at 19°S and 80°W-70.5°W at 01 UTC (a) and at 23 UTC (b). c) Meridional cross section at 71.5°W and 27.5°S-18°S at 18 UTC. Length of the arrow on top of each panel translates to 20m/s horizontal and 20m/min vertical wind speed.*

References:

Guan, B., and D. E. Waliser, 2015: Detection of atmospheric rivers: Evaluation and application of an algorithm for global studies, J. Geophys. Res. Atmos., 120, 12514-12535, doi:10.1002/2015JD024257

Acknowledgement:

The AR data were provided by Bin Guan via https://ucla.box.com/ARcatalog. Development of the AR detection algorithm and databases was supported by NASA.

c.boehm@uni-koeln.de